

# Analysis of Sampling and Quantization Effects on the Performance of PN Code Tracking Loops

Kevin J. Quirk and Meera Srinivasan  
Jet Propulsion Laboratory  
California Institute of Technology  
4800 Oak Grove Drive  
Pasadena, CA, 91109, USA

**Abstract**— Pseudonoise (PN) code tracking loops in direct-sequence spread-spectrum systems are often implemented using digital hardware. Performance degradation due to quantization and sampling effects is not adequately characterized by the traditional analog system feedback loop analysis. A low-complexity digital PN code tracking loop with one-bit non-commensurate sampling is analyzed, and the steady-state delay error variance is derived. The results are compared with that of an equivalent analog loop.

## I. INTRODUCTION

In order to extract data or timing information from a direct sequence spread spectrum (DS-SS) signal, one must know the phase of the received pseudonoise (PN) code with respect to a locally generated replica of the code. This process is divided into two stages: acquisition and tracking. Code acquisition consists of coarsely determining the received code phase (usually to within half a chip), while code tracking refines this estimate and maintains fine alignment between the received and local codes. The code tracking process is typically implemented as a tracking feedback loop; the performance of such a loop in its idealized form has been analyzed in [1] and [2]. Digital hardware implementation of these loops, however, introduces performance degradation through sampling and quantization that is not reflected in the standard analog loop analysis. In this paper we analyze the performance of one such reduced complexity loop, similar to that introduced by Thomas [3], which uses non-commensurate sampling (non-integer sample to chip time ratio) [4], one-bit analog-to-digital (A/D) conversion, and three level quantization of the carrier phase compensation signal.

A brief description of the use of one-bit non-commensurate sampling to achieve sub-sample timing accuracy will be given in Section II followed by the presentation and performance analysis of the code tracking loop in Sections III and IV. Optimization of this system for a given operating point is demonstrated in Section V along with a performance comparison with an equivalent analog code tracking loop.

## II. NON-COMMENSURATE SAMPLING

The sampling and quantization operations of an A/D converter are typically modeled as an integrate and dump circuit followed by a quantizer. If the integration time is significantly smaller than the sample time, we can simplify this model to that of an ideal sampler followed by a quantizer. If the sample

rate is an integer multiple of the chip rate, the timing resolution of the PN tracking system with an ideal sampler is limited to the sample time. This follows from observing that the sample positions of the received signal with respect to the chip transition positions are identical for each chip, and that in order for the sampled sequence resulting from one time offset to be discernible from the sampled sequence resulting from a different time offset (chip transition positions), a shift of up to one sample time may be required.

In order to achieve sub-sample-time discrimination in a PN tracking system using ideal sampling, a non-integer sample to chip time ratio can be used: this is referred to as non-commensurate sampling. By sampling the received signal and the local reference PN signal in this manner, sampled sequences that are potentially distinguishable at sub-sample time differences are created. To determine the achievable timing accuracy, both the smallest time offset that is guaranteed to introduce a difference in the sequences as well as the distinguishability of the sequences must be considered.

With non-commensurate sampling, while the sample positions with respect to the chip transition positions will differ from chip to chip, these positions are periodic and will eventually repeat. If the repetition occurs after  $N$  samples, there must be at least one chip transition difference between the sampled received and reference signals within this period; the minimum distinguishable time is thus  $T_c/N$ . The sample position period  $N$  is the smallest integer  $k$  such that  $k \cdot T_s = n \cdot T_c$ , where  $n$  is also an integer. Provided that  $T_c/T_s$  is not an irrational number, we can solve for the least integer  $k$  to obtain a timing accuracy of  $T_c/k$ . Note that if  $T_c/T_s$  is irrational the sample sequence never repeats and infinite accuracy is possible, given infinite time. However, as all sequence correlations would then be partial correlations this is not necessarily a desirable property.

While non-commensurate sampling allows increased timing accuracy, it also results in new sequences that do not possess the same correlation properties of the original PN sequence, and the ability to achieve this accuracy is compromised. The autocorrelation function of the sampled sequence is now given by

$$r(\tau_1, \tau_2) = \sum_{k=0}^N c_{\lfloor \frac{kT_s - \tau_1}{T_c} \rfloor} c_{\lfloor \frac{kT_s - \tau_2}{T_c} \rfloor}, \quad (1)$$

where  $\tau_1$  and  $\tau_2$  are the delays in the received and reference codes. Note that the sampled code sequences no longer have the cyclic shift properties that give rise to a dependence solely on the difference of the delays in the original code autocor-

The research described in this publication was carried out at the Jet Propulsion Laboratory, California Institute of Technology, under a contract with the National Aeronautics and Space Administration.

relation function; it is now a multi-variate function dependent on both delay positions. Figure 4 shows the autocorrelation function, (1), for a system with non-commensurate sampling of a maximal length shift register sequence of period  $M = 4095$  with  $T_c/T_s = 40001/20000$  (and hence sampled sequence period  $N = 40001$ ). Note that the autocorrelation function over this period is multi-valued; however, when plotted against  $\tau_2 - \tau_1$ , the effect is negligible. The choice of the sample to chip time ratio,  $T_c/T_s$ , and the length of the correlation time,  $N$ , control the degree to which the function is multi-valued and, given hardware constraints, can be chosen to minimize this spread to ensure the assumptions on the properties of the code sequence are approximately true.

### III. CODE TRACKING LOOP

The transmitted signal is a PN code waveform with rectangular chips of duration  $T_c$  modulating an RF carrier  $\omega_c$ . This signal is transmitted across the channel and received with a delay and reduced amplitude due to signal path loss. To model the thermal noise in the receiver front end an additive white Gaussian noise component with a flat double sided power spectrum  $N_o/2$  is added to the received signal. Assuming perfect frequency estimation and demodulation down to an intermediate frequency  $\omega_b$  that is much less than the chip rate, the received signal can be written in its low-pass equivalent form as

$$r(t) = \sqrt{2P} \sum_{n=-\infty}^{\infty} c_n p(t - nT_c - \tau) e^{j(\omega_b t + \psi)} + N(t) \quad (2)$$

where  $p(t)$  is a unit pulse of duration  $T_c$ , the delay  $\tau$  is uniformly distributed in  $[-T_c/2, T_c/2]$ , the phase offset  $\psi$  is uniformly distributed in  $[-\pi, \pi]$ ,  $N(t)$  is the complex low pass equivalent white Gaussian noise process with a flat power spectral density of  $2N_o$ , and  $P$  is the power of the transmitted signal.

Following the signal path of the receiver structure shown in Figure 1, the received signal is sampled at a rate  $1/T_s$ , which gives

$$r(kT_s) = \sqrt{2P} c_{\lfloor \frac{kT_s - \tau}{T_c} \rfloor} e^{j\theta_k} + N_k \quad (3)$$

where  $\theta_k = \omega_b(kT_s - \tau) + \psi$ ,  $N_k$  is a complex Gaussian noise process with a flat power spectral density of  $4N_oW$ , and  $W$  is the noise bandwidth of the front end. After sampling, one-bit quantization results in hard decisions being made on the real and imaginary parts independently. The hard decision outputs of the in-phase and quadrature-phase channels, denoted as  $I_k$  and  $Q_k$  respectively, may be written as

$$I_k = c_{\lfloor \frac{kT_s - \tau}{T_c} \rfloor} \cdot e_k^I \quad \text{and} \quad Q_k = c_{\lfloor \frac{kT_s - \tau}{T_c} \rfloor} \cdot e_k^Q \quad (4)$$

where  $e_k^I$  and  $e_k^Q$  take on unity for a correct decision and negative one if an error has been made.

As we are primarily interested in the steady state performance of the tracking loop we assume that both fine frequency estimation as well as carrier phase estimation are made using the in-phase and quadrature-phase values of a code correlation concurrently with or prior to the convergence state of the code tracking loop. We will therefore assume perfect frequency and phase estimates are available.

After the hard decision, the frequency and phase offset is compensated for by weighting the in-phase and quadrature-phase channels hard decisions,  $\hat{I}_k$  and  $\hat{Q}_k$ , by the three-level quantized phase compensation functions  $f_I(\theta_k)$  and  $f_Q(\theta_k)$ , where

$$f_I(\theta) = \begin{cases} 0 & \frac{3}{4}\pi - \alpha \leq \theta < \frac{3}{2}\pi + \alpha \\ 1 & \frac{3}{2}\pi + \alpha \leq \theta < \frac{3}{4}\pi - \alpha \\ 0 & \frac{\pi}{2} - \alpha \leq \theta < \frac{\pi}{2} + \alpha \\ -1 & \frac{\pi}{2} + \alpha \leq \theta < \frac{3}{2}\pi - \alpha \end{cases}$$

and  $f_Q(\theta) = f_I(\theta + \pi/2)$ , where  $\alpha \in (0, \pi/4)$  is set for the particular system. This weighting corrects sign changes due to the phase offset and removes the decisions with the highest error probability. As we have assumed frequency and phase synchronization the real component of  $(\hat{I}_k + j\hat{Q}_k) \cdot (f_I(\theta_k) - jf_Q(\theta_k))$  forms our test statistic

$$\begin{aligned} g &= \Re\{(\hat{I}_k + j\hat{Q}_k) \cdot (f_I(\theta_k) - jf_Q(\theta_k))\} \\ &= f_I(\theta_k)\hat{I}_k + f_Q(\theta_k)\hat{Q}_k. \end{aligned}$$

Note that when  $\theta_k$  falls within  $[-\alpha, \alpha]$ ,  $\hat{I}_k$  is weighted by 1 and  $\hat{Q}_k$  is weighted by zero. When  $\theta_k$  is in  $[\alpha, \frac{\pi}{2} - \alpha]$  both  $\hat{I}_k$  and  $\hat{Q}_k$  are weighted by unity. Similarly when  $\theta_k$  is in  $[\pi - \alpha, \pi + \alpha]$ ,  $\hat{I}_k$  is weighted by  $-1$ , to account for the sign change in that region, and  $\hat{Q}_k$  is weighted by zero, since it has a high probability of error. There are eight such regions of  $\theta_k$ :

$$\begin{aligned} R_1 &= [-\alpha, \alpha] & R_5 &= [\pi - \alpha, \pi + \alpha] \\ R_2 &= [\alpha, \pi/2 - \alpha] & R_6 &= [\pi + \alpha, 3\pi/2 - \alpha] \\ R_3 &= [\pi/2 - \alpha, \pi/2 + \alpha] & R_7 &= [3\pi/2 - \alpha, 3\pi/2 + \alpha] \\ R_4 &= [\pi/2 + \alpha, \pi - \alpha] & R_8 &= [3\pi/2 + \alpha, 2\pi - \alpha] \end{aligned}$$

Since we have phase synchronization, a phase induced sign change is compensated for by the weighting function and is therefore not an error. Incorporating this into the test statistic we write

$$g_k = c_{\lfloor \frac{kT_s - \tau}{T_c} \rfloor} |f_I(\theta_k)| e_k^I + c_{\lfloor \frac{kT_s - \tau}{T_c} \rfloor} |f_Q(\theta_k)| e_k^Q,$$

where  $e_k^I$  and  $e_k^Q$  are hard decision errors which are dependent only on the magnitude of  $\cos(\theta_k)$  and  $\sin(\theta_k)$  respectively, in addition to the received signal power and noise.

After frequency and phase compensation, correlations of the test statistics  $\{g_k\}$  with early and late time shifts of the sampled despreading code,  $c(kT_s - \hat{\tau} + T_c/2)$  and  $c(kT_s - \hat{\tau} - T_c/2)$  respectively, are formed, where  $\hat{\tau}$  is the estimate of the path delay  $\tau$ . Using the sequence formed by sampling the early code sequence, the early correlation value  $\gamma_e$  is given by

$$\gamma_e = \sum_{k=0}^N r_k^e \left[ |f_I(\theta_k)| e_k^I + |f_Q(\theta_k)| e_k^Q \right]$$

where  $r_k^e = c_{\lfloor \frac{kT_s - \hat{\tau} + T_c/2}{T_c} \rfloor} c_{\lfloor \frac{kT_s - \tau}{T_c} \rfloor}$  represents the resulting sequence if there were no errors. Separating the sum into regions of  $\theta_k$  gives us

$$\gamma_e = \sum_{\theta_k \in R_1 \cup R_5} r_k^e e_k^I + \sum_{\theta_k \in R_3 \cup R_7} r_k^e e_k^Q + \sum_{\theta_k \in R_2 \cup R_4 \cup R_6 \cup R_8} r_k^e \left[ e_k^I + e_k^Q \right].$$

If  $1/\omega_b \ll NT_s$  and  $\frac{\omega_b}{s} \notin Z^+$ , then over the sum interval  $\theta_k$  will be evenly distributed throughout  $[0, 2\pi)$ , and the following cardinalities will hold:

$$\begin{aligned} |\{\theta_k\} \text{ s.t. } \theta_k \in R_1 \cup R_5\} &\approx 2 \cdot \frac{2\alpha}{2\pi} N \triangleq \beta N/2, \\ |\{\theta_k\} \text{ s.t. } \theta_k \in R_3 \cup R_7\} &\approx 2 \cdot \frac{2\alpha}{2\pi} N = \beta N/2, \\ |\{\theta_k\} \text{ s.t. } \theta_k \in R_2 \cup R_4 \cup R_6 \cup R_8\} &\approx 4 \cdot \frac{\frac{\pi}{2} - 2\alpha}{2\pi} N \\ &= (1 - \beta)N \end{aligned}$$

where  $\beta = 4\alpha/\pi$ . As reordering the elements of the sum does not effect the result we can write

$$\gamma_e = \sum_{k=0}^{\beta N/2-1} r_k^e e_k^I + \sum_{k=\beta N/2}^{\beta N-1} r_k^e e_k^Q + \sum_{k=\beta N}^{N-1} r_k^e [e_k^I + e_k^Q]. \quad (5)$$

In the first and second sums, as the in-phase and quadrature channels result from a symmetric bandpass channel,  $e_I$  and  $e_Q$  are identically distributed and each have a probability of error of

$$\begin{aligned} \rho_1 &\triangleq \Pr(e_k^I = -1) = \Pr(e_k^Q = -1) \\ &= \frac{1}{2\alpha} \int_{-\alpha}^{\alpha} \phi\left(-\sqrt{\frac{P}{WN_o}} \cos(\theta)\right) d\theta \end{aligned}$$

where we have assumed a uniform distribution of  $\theta_k$ , which can be justified from the  $\tau\omega_b$  term within  $\theta_k$ , and where  $\phi(\cdot)$  is the cumulative distribution function of zero mean unit variance Gaussian random variable. In the third sum,  $e_k^I$  and  $e_k^Q$  are also i.i.d. and each have a probability of error of

$$\begin{aligned} \rho_2 &\triangleq \Pr(e_k^I = -1) = \Pr(e_k^Q = -1) \\ &= \frac{1}{\pi/2 - 2\alpha} \int_{\alpha}^{\pi/2 - \alpha} \phi\left(-\sqrt{\frac{P}{WN_o}} \cos(\theta)\right) d\theta. \end{aligned}$$

The density function of  $\gamma_e$  can be found directly by counting the number of sign flips in the sum along with their probabilities. However, analysis with the resulting density is difficult. We therefore use the central-limit theorem to approximate the density of  $\gamma_e$ . To invoke the central limit theorem the errors must be independent. The test statistic from which the error results is dependent upon both the thermal noise and  $\cos(\theta_k)$  in the mean term. As the random component of  $\theta_k$  is  $\omega_b\tau + \psi$ , which does not change from sample to sample, the samples would appear to not be independent. However, with the assumption that the thermal noise is the dominant factor in the test statistic (negative SNR), we can model the errors as independent from sample to sample. Therefore, for large  $N$  the central limit theorem can be invoked and the density of  $\gamma_e$  is Gaussian with mean

$$E[\gamma_e] = (1 - 2\rho_1) \sum_{k=0}^{\beta N-1} r_k^e + 2(1 - 2\rho_2) \sum_{k=\beta N}^{N-1} r_k^e. \quad (6)$$

Assuming  $N$  is large enough to allow us to approximate the auto-correlation sequence  $r(\tau, \hat{\tau})$  as  $r(\tau - \hat{\tau})$  we can write

$$\begin{aligned} r_e(\tau - \hat{\tau} + T_c/2) &= \sum_{k=0}^{N-1} r_k^e = \left[ N - \left\lfloor \frac{N(\tau - \hat{\tau} + T_c/2)}{T_c} \right\rfloor \right] \\ &\approx \frac{N}{2} - \frac{N(\tau - \hat{\tau})}{T_c} \end{aligned}$$

where we have used  $|\tau - \hat{\tau}| \leq T_c/2$ . As  $N$  is very large, we assume that the partial autocorrelation value may be obtained by scaling the autocorrelation function above, so that

$$\begin{aligned} E[\gamma_e] &= (1 - 2\rho_1) \left[ \frac{\beta N}{2} - \frac{\beta N(\tau - \hat{\tau})}{T_c} \right] \\ &+ 2(1 - 2\rho_2) \left[ \frac{(1 - \beta)N}{2} - \frac{(1 - \beta)N(\tau - \hat{\tau})}{T_c} \right]. \end{aligned}$$

Following a similar procedure the variance is given by

$$\text{Var}(\gamma_e) = 4N[\beta\rho_1(1 - \rho_1) + 2(1 - \beta)\rho_2(1 - \rho_2)].$$

Similarly,  $\gamma_I$  is a Gaussian random variable with

$$\begin{aligned} E[\gamma_I] &= (1 - 2\rho_1) \left[ \frac{\beta N}{2} + \frac{\beta N(\tau - \hat{\tau})}{T_c} \right] \\ &+ 2(1 - 2\rho_2) \left[ \frac{(1 - \beta)N}{2} + \frac{(1 - \beta)N(\tau - \hat{\tau})}{T_c} \right] \end{aligned}$$

and  $\text{Var}(\gamma_I) = \text{Var}(\gamma_e)$ . Note that the independence of  $\gamma_e$  and  $\gamma_I$  can be shown by demonstrating that their their cross moment factors. One can also show that successive values of  $\gamma_e$  and  $\gamma_I$  are independent; they are white processes.

#### IV. LOOP ANALYSIS

The code tracking loop uses the difference between the early and late correlations to form an estimate of the delay  $\epsilon_m \triangleq \tau - \hat{\tau}_m$ ; this difference is

$$\hat{s}_m(\epsilon_m) = \gamma_I - \gamma_e = C\epsilon_m + N_m \quad (7)$$

where  $C \triangleq [(1 - 2\rho_1)\beta + 2(1 - 2\rho_2)(1 - \beta)]2N/T_c$  and where  $N_m$  is a zero mean Gaussian process with a flat spectral density of  $8N[\beta\rho_1(1 - \rho_1) + 2(1 - \beta)\rho_2(1 - \rho_2)]$ .

The code tracking loop can then be formulated as a discrete time linear feedback loop, as shown in the Figure 2 (note there is no loop filter). The input to the loop is  $C\tau_m + N_m$ , from which the delay estimate,  $C\hat{\tau}_m$  is subtracted. The resulting quantity is then multiplied by a gain,  $G_d$ , and accumulated to form the estimate  $\hat{\tau}_{m+1}$ , which is applied on the next loop update. The error in the estimate can therefore be written as

$$\epsilon_m = \epsilon_{m-1} - G_d [C\epsilon_{m-1} + N_{m-1}].$$

Assuming that both  $\epsilon_m$  and  $N_m$  are wide sense stationary second order processes we can write them in terms of their orthogonal

increment process spectral representations [5] and solve for the variance of the process as

$$\sigma_{\epsilon}^2 = 8N[\beta\rho_1(1-\rho_1) + 2(1-\beta)\rho_2(1-\rho_2)] \cdot \frac{1}{2\pi} \int_{-\pi}^{\pi} \left| \frac{G_d e^{-j\lambda}}{1 - (1 - G_d C) e^{-j\lambda}} \right|^2 d\lambda \quad (8)$$

with the stability constraint

$$G_d < \frac{T_c}{N[(1-2\rho_1)\beta + 2(1-2\rho_2)(1-\beta)]}$$

In order to avoid oscillatory behavior, we restrict  $G_d$  to half of the constraint value. The integral in (8) can be solved by transforming it to the complex domain and performing a contour integration around the unit circle, resulting in

$$\sigma_{\epsilon}^2 = \frac{G_d^2 8N[\beta\rho_1(1-\rho_1) + 2(1-\beta)\rho_2(1-\rho_2)]}{1 - \left(1 - G_d[(1-2\rho_1)\beta + 2(1-2\rho_2)(1-\beta)]2\frac{N}{T_c}\right)^2} \quad (9)$$

Note that performance of the loop is parameterized by the phase compensation parameter  $\beta$ ; an optimization of this parameter to minimize  $\sigma^2$  is therefore possible for a given sample SNR or operating range.

## V. COMPARISON WITH AN ANALOG LOOP

The use of sampling and quantization in a digital code tracking loop results in a performance penalty when compared to that of the ideal analog loop. The criterion for equivalence between the digital and analog loops will be that their respective transfer functions have the same order and 3dB point. From Section IV we note that the transfer function of the digital loop is dependent upon the operating point of the loop, which is the sample SNR, as well as the value of the loop parameter  $\beta$ ; matching the loop bandwidth of the digital loop with the analog loop will therefore require selection of the loop parameters with regard to the operating point of the receiver. We first consider the performance of the equivalent analog code tracking loop.

A first order baseband analog code tracking loop is shown in Figure 3. The input signal is written in its low-pass equivalent form as

$$r(t) = \sqrt{2P} \sum_{n=-\infty}^{\infty} c_n p(t - nT_c - \tau) + N(t)$$

where  $N(t)$  is a complex Gaussian process with a power spectral density of  $2N_o$ . Note that without the hard decision operation of the digital loop there is no need for the frequency offset and the signal can be brought completely down to baseband. The transfer function of this loop, ignoring the self interference noise [6, p. 155], can be written as

$$H(s) = \frac{G_a}{s + \frac{G_a \sqrt{P}}{T_c} \left(1 + \frac{1}{M}\right)} \quad (10)$$

where  $M$  is the period of the spreading code.

Unlike the digital loop, the analog transfer function is not a function of the operating point of the receiver. Again using the spectral representations of the processes, the variance of the estimation error can be written as

$$\sigma^2 = \frac{G_a T_c N_o}{4\sqrt{P}},$$

where we have assumed the front end bandwidth  $W$  is much greater than the tracking loop bandwidth.

In order to compare the performance of the analog and digital loops we require them to have equivalent bandwidths. From (10), the 3dB bandwidth of the analog loop is given by

$$\omega_o = G_a \frac{2\sqrt{P}}{T_c} \left(1 + \frac{1}{M}\right).$$

Using (8), the 3dB bandwidth of the digital loop is given by

$$\omega_o = \cos^{-1} \left( \frac{4a - a^2 - 1}{2a} \right) \cdot \frac{1}{NT_s}$$

where  $a \triangleq 1 - G_d C$ . As previously noted, the analog loop bandwidth is dependent only on the loop parameter  $G_a$ , while the bandwidth of the digital loop is parameterized by the receiver operating point through  $\rho_1$  and  $\rho_2$ , the phase compensation parameter  $\beta$ , and the loop gain parameter  $G_d$ . To obtain equivalent loops for each operating point, we first choose  $\alpha$  by optimizing the error variance over  $\alpha \in (0, \pi/4)$  (corresponding to  $\beta \in (0, 1)$ ), and then choose  $G_d$  to match the bandwidth with that of the analog loop.

The effects of both sampling and quantization in the digital code loop can be elucidated by comparing the digital and analog code loop performances in different receiver scenarios. First consider a receiver with a front end noise bandwidth equal to the chip rate,  $W = 2\pi/T_c$ . For the digital code tracking loop the optimal choice of the phase compensation parameter is found by minimizing (9) with respect to  $\beta$  at each operating SNR,  $(P/N_o W)$ . Figure 5 contains a plot of the optimal values of  $\alpha$  versus  $P/N_o W$  for a correlation time of  $N = 81902$  samples. Using these optimal values of  $\alpha$  and the receiver operating point the 3dB points of both the analog and digital loops are equated and their respective error variance performances are plotted in Figure 6 versus  $P/N_o$  for code loop bandwidths of 10Hz and 100Hz. For both loop bandwidths, 10Hz and 100Hz, the digital code loop with its non-commensurate sampling and hard decisions suffered approximately 2dB in performance relative to the idealized analog code loop. As the receiver front end noise bandwidth is equal to the chip-rate, the effects from the quantization are the dominating factors in the performance loss. To illustrate the effects of the sampling consider a receiver without a good anti-aliasing filter, say one having a front end noise bandwidth of twice the chip rate. As the hard decisions in the digital system are made at this much lower SNR the performance is greatly reduced relative to the analog system whose performance is independent of the receiver front end bandwidth. This is also illustrated in Figure 6 for a loop bandwidth of 10Hz which shows a 6dB performance loss relative to the analog loop.

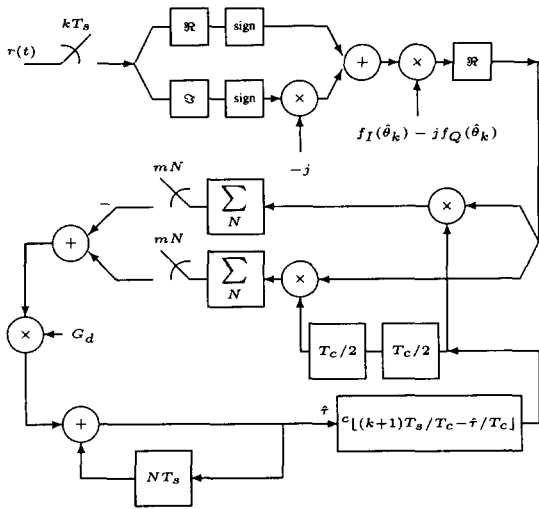


Fig. 1. Low-pass equivalent digital code tracking loop.

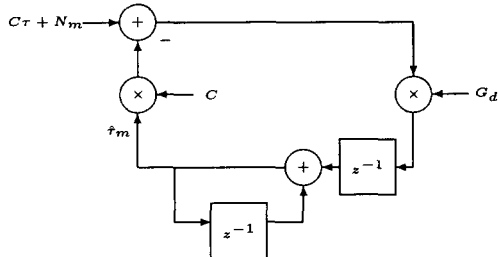


Fig. 2. Analytical depiction of the digital code tracking loop.

## VI. CONCLUSIONS

The methodology for analytically evaluating the performance of a digital code tracking loop in terms of steady-state delay error variance using non-commensurate sampling and hard decisions was described. The analysis showed that the loop bandwidth of the digital loop is dependent upon the operating point of the receiver, and that optimization of the phase compensation signal with respect the operating point of the loop is possible. A comparison between the digital code tracking loop and an equivalent analog loop was made for various operating scenarios allowing for an assessment of the performance cost of the non-commensurate sampling and hard decision quantization.

## REFERENCES

- [1] Heinrich Meyr, "Delay-lock tracking of stochastic signals," *IEEE Transactions on Communications*, vol. 24, no. 3, pp. 331-339, March 1976.
- [2] Andreas Polydoros and Charles L. Weber, "Analysis and optimization of correlative code-tracking loops in spread-spectrum systems," *IEEE Transactions on Communications*, vol. 33, no. 1, pp. 30-43, January 1985.
- [3] J. B. Thomas, "Signal-processing theory for the TubroRogue receiver," *Publication 95-6, Jet Propulsion Laboratory*, April 1995.
- [4] A. Mileant, S. Million, S. Hinedi, and U. Cheng, "The performance of the all-digital data transition tracking loop using nonlinear analysis," *IEEE Transactions on Communications*, vol. 43, no. 2/3/4, pp. 1202-1215, February/March/April 1995.
- [5] P. J. Brockwell and R. A. Davis, *Time Series: Theory and Methods*, Springer, New York, NY, 2nd edition, 1991.
- [6] Roger L. Peterson, Rodger Ziemer, and David Borth, *Introduction to Spread Spectrum Communications*, Prentice Hall, Inc., Upper Saddle River, N.J., 1995.

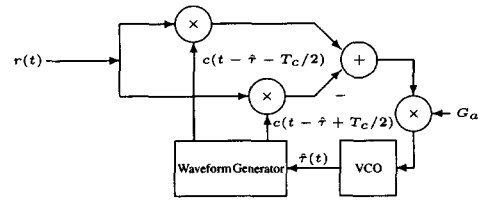


Fig. 3. Low-pass equivalent analog code loop

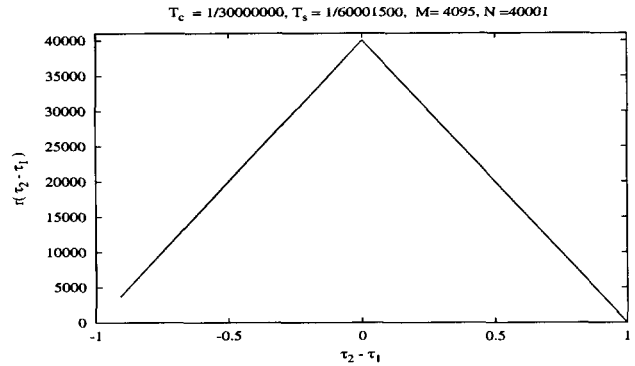


Fig. 4. The autocorrelation function of the sampled PN code.

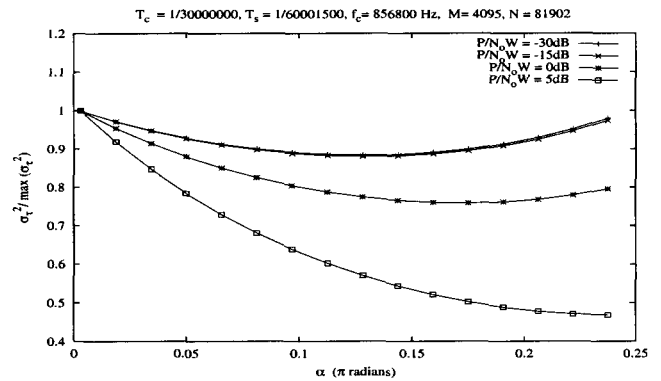


Fig. 5. The normalized variance versus the phase angle threshold  $\alpha$ .

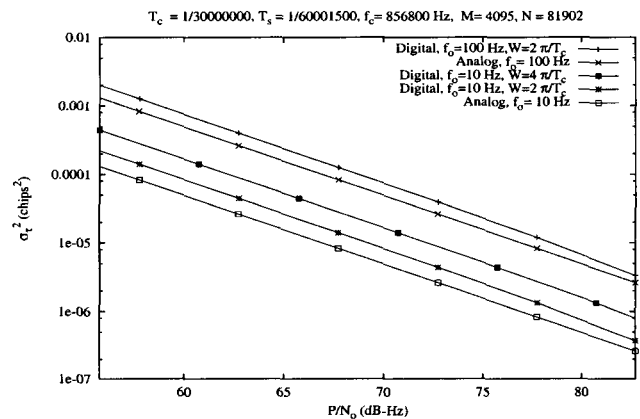


Fig. 6. The variance of the delay error,  $\sigma_{\tau_d}^2$ , for both analog and digital code tracking loops.